Published in final edited form as:
J Cereb Blood Flow Metab. 2009 January ; 29(1): 10–18. doi:10.1038/jcbfm.2008.97.

New insights into central roles of cerebral oxygen metabolism in the resting and stimulus-evoked brain

Xiao-Hong Zhu, **Nanyin Zhang**, **Yi Zhang**, **Kâmil Uğurbil**, and **Wei Chen**
Center for Magnetic Resonance Research, Department of Radiology, University of Minnesota Medical School, Minneapolis, Minnesota, USA

Abstract

The possible role of oxygen metabolism in supporting brain activation remains elusive. We have used a newly developed neuroimaging approach based on high-field *in vivo* ^{17}O magnetic resonance spectroscopic (MRS) imaging to noninvasively image cerebral metabolic rate of oxygen ($CMRO_2$) consumption in cats at rest and during visual stimulation. It was found that $CMRO_2$ increases significantly (32.3%±10.8%, $n = 6$) in the activated visual cortical region as depicted in blood oxygenation level dependence functional maps; this increase is also accompanied by a $CMRO_2$ decrease in surrounding cortical regions, resulting a smaller increase (9.7%±1.9%) of total $CMRO_2$ change over a larger cortical region displaying either a positive or negative $CMRO_2$ alteration. Moreover, a negative correlation between stimulus-evoked percent $CMRO_2$ increase and resting $CMRO_2$ was observed, indicating an essential impact of resting brain metabolic activity level on stimulus-evoked percent $CMRO_2$ change and neuroimaging signals. These findings provide new insights into the critical roles of oxidative metabolism in supporting brain activation and function. They also suggest that *in vivo* ^{17}O MRS imaging should provide a sensitive neuroimaging modality for mapping $CMRO_2$ and its change induced by brain physiology and/or pathologic alteration.

Keywords

brain activation; cerebral metabolic rate of oxygen; functional MRI; *in vivo* ^{17}O MRS; imaging $CMRO_2$

Introduction

Normal brain function requires large amounts of energy. This high energy demand is met mainly through the chemical process of oxidative phosphorylation in the brain mitochondria to produce adequate quantities of adenosine triphosphate (ATP; Attwell and Laughlin, 2001; Du *et al*, 2008; Hyder *et al*, 2006; Lei *et al*, 2003; Raichle, 1987; Sokoloff, 1991). Under the resting condition, this process is responsible for the consumption of most glucose used by the brain, generating ~36 ATPs from each glucose molecule. It is also tightly coupled to cerebral oxygen utilization and is responsible for ~20% of the total oxygen consumption in the human body even though the brain constitutes only ~2% of the body weight. Therefore, the cerebral oxidative metabolism is essential for supplying brain energy and supporting brain function. Consequently, cerebral metabolic rate of oxygen ($CMRO_2$) consumption provides an important physiologic parameter that can be used to evaluate cerebral bioenergetics in healthy and

Correspondence: Dr X-H Zhu or Dr W Chen, Center for Magnetic Resonance Research, Department of Radiology, University of Minnesota, 2021 6th Street SE, Minneapolis, MN 55455, USA. E-mail: zhu@cmrr.umn.edu or wei@cmrr.umn.edu.

Conflict of interest
The authors declare no competing financial interests.

diseased brains at rest; as well as to investigate the functional neurometabolic relation during brain stimulation and/or task performance. However, the ability to directly and reliably image resting $CMRO_2$ and $CMRO_2$ alteration during brain activation has been a major challenge for several decades. Positron emission tomography (PET) combined with ^{15}O radiotracers has been perhaps the only established *in vivo* imaging method able to directly image $CMRO_2$ (Ibaraki *et al*, 2008; Mintun *et al*, 1984; Mintun *et al*, 2002). Despite its relatively coarse spatial resolution, its requirement for complex mathematical modeling, and the involvement of multiple measurement procedures (Mintun *et al*, 1984), the ^{15}O-PET technique has been applied to investigate oxygen metabolism in the human brain under various conditions. In one prominent PET application, regional stimulus-evoked $CMRO_2$ change in the human visual cortex was determined to be ~5% whereas alterations in cerebral blood flow (CBF) and cerebral metabolic rate of glucose (CMR_{glc}) consumption were significantly higher (~50%; Fox *et al*, 1988). These metabolic rate changes only corresponded to ~7% increase in the stimulus-evoked ATP production rate, a surprising finding implying that energy cost of stimulus-evoked neuronal activity is relatively small and it might be met partially through the glycolysis process in the awake human brain (Barinaga, 1997; Fox *et al*, 1988; Raichle and Mintun, 2006). In contrast, the cerebral oxidative glucose consumption rate, determined through the *in vivo* ^{13}C magnetic resonance spectroscopic (MRS) measurement, was reported to increase substantially up to 80%–100% in the anesthetized rat somatosensory cortex during forepaw electric stimulation (Hyder *et al*, 2001). One possible source of this sizable discrepancy has been speculated to be the difference in baseline $CMRO_2$ levels between the awake human and the anesthetized rat brains, highlighting the importance of quantitative $CMRO_2$ measurements under both baseline and stimulated brain states.

Qualitatively, the finding that the ratio between the stimulus-evoked percent $CMRO_2$ change versus that of CBF or CMR_{glc} is much smaller than 1 (Fox *et al*, 1988) is consistent with and underlies the interpretation of the blood oxygenation level dependence (BOLD) contrast (Ogawa *et al*, 1990; Raichle and Mintun, 2006) detected by functional magnetic resonance imaging (fMRI), which has become the most prominent neuroimaging modality for mapping brain activation (e.g., Bandettini *et al*, 1992; Kwong *et al*, 1992; Ogawa *et al*, 1992). However, fMRI is unable to directly detect neuronal activity; instead, it relies on a complex interplay among CBF, cerebral blood volume (CBV), and $CMRO_2$ changes induced by altered brain activity (Ogawa *et al*, 1993). Precise interpretation of fMRI results requires a better understanding of the quantitative relationship between the fMRI BOLD contrast and the underlying neurophysiology—in particular the stimulus-evoked $CMRO_2$ change.

Therefore, the ability to image absolute $CMRO_2$ with relatively high spatial resolution and temporal resolution is crucial towards understanding cerebral metabolic events that occur during brain activation, and their implication on quantifying neuroimaging signals. Towards this goal, we recently established the three-dimensional (3D) ^{17}O magnetic resonance spectroscopy imaging (MRSI) method at high/ultra-high magnetic fields (Zhu *et al*, 2002; Zhu *et al*, 2007) as a noninvasive neuroimaging modality for imaging $CMRO_2$ *in vivo*; and have rigorously evaluated this method using an animal model (Zhang *et al*, 2004; Zhu *et al*, 2007). This $CMRO_2$ imaging method relies on detecting the dynamic change of ^{17}O-labeled metabolic water ($H_2\,^{17}O$) produced by oxygen metabolism in the brain mitochondria during a short (2 to 3 mins) inhalation of ^{17}O-isotope-labeled oxygen gas (Arai *et al*, 1990; Mateescu *et al*, 1989; Pekar *et al*, 1991; Zhu *et al*, 2005; Zhu *et al*, 2002; Zhu *et al*, 2007). In the present study, we exploit this newly developed high-field *in vivo* ^{17}O MRSI approach to study the possible roles of cerebral oxygen metabolism in brain function and stimulus-evoked activation by imaging $CMRO_2$ in the cat primary visual cortex (V1; cortical areas 17 and 18) at rest (defined as baseline condition) and during visual stimulation, ultimately generating functional metabolic activation maps of relative $CMRO_2$ change (i.e., $\Delta CMRO_2/CMRO_2$ maps) and comparing them with the BOLD-based fMRI mapping results. The overall results provide new insights

into quantitative relationship of $CMRO_2$ in a resting visual cortex and its change evoked by visual stimulation; they also provide vital evidence to potentially coincide several long-standing and unsolved issues in the literature regarding the quantitative relationships among $CMRO_2$, brain energy expenditure, cerebral bioenergetics, and brain activation.

Materials and methods

Animal Preparation

Five female adolescent cats were used to conduct this study. Cats were initially anesthetized with a mixture of ketamine (15.0 mg/kg) and xylazine (2.5 mg/kg). After oral intubation, mechanical ventilation (30 to 33 stokes/mins) was applied and anesthesia was switched to 0.9% to 1.2% isoflurane (~1.5MAC) in a N_2O/O_2 mixture of 70:30 volume ratio throughout the experiment. The pupils of the cat were dilated with atropine sulfate solution; corrective contact lenses were placed to focus the eyes on the visual stimulus by refracting and locating the fovea of the cat retina with the aid of a fundus camera (Zeiss, Jena, Germany). The visual stimulus was a binocular high-contrast square-wave moving and rotating gratings (0.3 cycle/deg, 2 cycles/sec, and 16° rotation for every 4 secs) to achieve optimal visual stimulation of the neurons with different orientation preferences in the cat primary visual cortex. The cats were placed in a cradle with head position restrained by the mouth and ear bars. The animal physiologic condition was continuously monitored and maintained during the entire experiment. All animal surgical procedures and experimental protocol were approved by the Institutional Animal Care and Use Committee of the University of Minnesota.

Magnetic Resonance Spectroscopy Imaging and Magnetic Resonance Imaging Measurements

The ^{17}O MRSI and ^{1}H MRI measurements were conducted on a 9.4T horizontal animal magnet (Magnex Scientific, Oxford, UK) interfaced with a Varian INOVA console (Varian Inc., Palo Alto, CA, USA). A radiofrequency (RF) probe consisted of a ^{17}O surface coil covering the cat V1 region for acquiring ^{17}O MRSI and a larger ^{1}H coil for brain anatomic images and fMRI was used in this study.

^{17}O Magnetic Resonance Spectroscopy Imaging for Imaging Cerebral Metabolic Rate of Oxygen—The spatial localization of ^{17}O MRSI was achieved by using the 3D Fourier series window chemical shift imaging approach with a total acquisition time of 12.5 secs per MRSI volume (Hendrich *et al*, 1994; Zhu *et al*, 2002). Other ^{17}O acquisition parameters were: $3 \times 3 \times 2.5$ cm^3 field-of-view (FOV); $9 \times 9 \times 5$ phase encodes; 12 μL voxel size, which is corresponding to a nominal voxel size of 43 μL. A $17 \times 17 \times 9$ matrix of ^{17}O free induced decay signals were generated from the original $9 \times 9 \times 5$ phase encoded raw image data for generating each 3D ^{17}O MRSI dataset.

Two paired measurements for collecting series of 3D ^{17}O MRSI before and during 2 to 3 mins inhalation of $^{17}O_2$ gas (up to 89% ^{17}O enrichment purchased from ISOTEC Inc, Miamisburg, OH, USA) were performed for each cat in the absence and presence of visual stimulation, respectively; and only Cat 5 had repeated twice the paired ^{17}O MRSI measurements in the same experimental session to test the reproducibility and reliability of the $CMRO_2$ imaging approach.

The natural abundant ^{17}O signal of brain water obtained before the $^{17}O_2$ gas inhalation was used as internal reference for quantifying the absolute metabolic H_2 ^{17}O concentration in the brain; and the dynamic change of the metabolic H_2 ^{17}O concentration obtained during $^{17}O_2$ gas inhalation was applied to determine $CMRO_2$ using the linear regression model and to generate 3D $CMRO_2$ images (Zhang *et al*, 2004; Zhu *et al*, 2002; Zhu *et al*, 2007). The

functional $CMRO_2$ activation maps were created based on the value of $\Delta CMRO_2/CMRO_2$, in which $\Delta CMRO_2$ represents the difference between the stimulated and control $CMRO_2$ values.

Two criterions were applied to quantify the $CMRO_2$ values measured under resting and stimulated conditions, as well as $\Delta CMRO_2/CMRO_2$. The ^{17}O RF surface coil used in this study provides optimal sensitivity for detecting the ^{17}O MRSI signal in the cat V1 and surrounding brain regions. In contrast, the detected ^{17}O signal intensity reduces substantially in the brain regions, which are distant from the RF coil, resulting in a low signal-to-noise ratio (SNR). Thus, the first criterion was to exclude the ^{17}O MRSI voxels with low SNR of natural abundance brain water signal from further $CMRO_2$ quantification. The averaged SNR from the ^{17}O MRSI voxels, which were included in $CMRO_2$ quantification was approximately 10:1. The Monte Carlo simulation (unpublished results) has suggested that the $CMRO_2$ fitting error measured by the high-field ^{17}O MRSI approach can reach a few percents if the SNR of natural abundance brain water signal is below 10:1. Thus, the second criterion was to set a threshold of $-5\% > \Delta CMRO_2/CMRO_2 > 5\%$ for calculating the stimulus-evoked percent $CMRO_2$ change (i.e., $\Delta CMRO_2/CMRO_2$); and generating the functional metabolic activation maps of $\Delta CMRO_2/CMRO_2$.

The functional $\Delta CMRO_2/CMRO_2$ maps were further analyzed in two ways. The first way was to average the baseline and stimulated $CMRO_2$ value, respectively, only from the same brain regions showing a positive stimulus-evoked $CMRO_2$ change; and these averaged $CMRO_2$ values were further used to calculate the averaged value of positive $\Delta CMRO_2/CMRO_2$. The second way was to calculate the baseline and stimulated $CMRO_2$ value, respectively, averaged from the brain regions showing either a positive or a negative stimulus-evoked $CMRO_2$ change; and these $CMRO_2$ values were used to present the averaged value of net change of $\Delta CMRO_2/CMRO_2$ in these brain regions.

Functional Magnetic Resonance Imaging Mapping—At first, multislice anatomic images were acquired using a conventional T_1-weighted imaging method. On the basis of these anatomic images, slices covering the cat V1 areas were appropriately selected for acquiring fMRI data using multislice gradient echo planar images (EPI) with the following acquisition parameters: repetition time (TR) = 1.65 sec; echo time (TE) = 19 ms; five adjacent axial EPI slices; FOV= 5×5 cm^2; 780 μm × 780 μm in-plane spatial resolution; 1 mm slice thickness and 2 to 2.5 mm interval between adjacent slices.

The fMRI measurements were based on the block paradigm design: three control and two task periods in an interleaved way. Activation maps were generated using a time-shifted cross-correlation method (Bandettini *et al*, 1992; Xiong *et al*, 1995). The activated pixels were identified by correlating the fMRI time course with a trapezoidal function (the modified box-car function with the capability of accounting for hemodynamic delays). This procedure generated typical activation maps in V1, which were consistent across different cats. We chose a statistical threshold of $P < 0.01$ to generate fMRI activation maps.

The paired *t*-test was performed for statistical analysis and the results are presented as mean ± s.d.

Results, Discussion, and Conclusions

Stimulus-Evoked Cerebral Metabolic Rate of Oxygen Increase During Brain Activation

Figure 1 shows the 3D images of absolute $CMRO_2$ values obtained at rest and during visual stimulation, functional metabolic activation maps of $\Delta CMRO_2/CMRO_2$, BOLD-based fMRI maps, and their corresponding brain anatomic images in four adjacent image slices chosen from 3D image data in a representative cat brain. This figure clearly illustrates a significant

$CMRO_2$ increase in the activated brain region in the cat visual cortex (defined as activated V1 region herein) in response to a full-field, binocular grating visual stimulation. The size and location of the activated brain regions depicted in the functional $\Delta CMRO_2/CMRO_2$ maps largely coincide with those regions determined by fMRI maps showing positive BOLD changes in the same cat brain despite of different spatial resolutions between $CMRO_2$ and BOLD functional images. Figure 2 shows the absolute $CMRO_2$ values averaged over these activated brain regions in different image slices from one representative cat, and the summarized results of six measurements from five cats (one cat having two repeated measurements under control and stimulated conditions). The $CMRO_2$ value averaged spatially from the activated cat V1 region showing a positive change of $\Delta CMRO_2/CMRO_2$ was 1.26 ± 0.09 μmol/g per min (n = 6) under the visual stimulation condition; and this value is significantly higher than that of 0.97 ± 0.04 μmol/g per min (n = 6) measured at resting condition from the same brain region, indicating a 32.3% ± 10.8% increase of $CMRO_2$ in the activated V1 region ($P < 0.005$, paired t-test). Figures 3A and 3B summarize the intersubject averaged $CMRO_2$ results measured under resting and stimulated brain states, indicating a substantial $CMRO_2$ increase ranging approximately from 20% to 50% in the activated V1 region in different cats studied (see Figure 3B). These results suggest that the oxidative metabolic activity is significantly elevated in the anesthetized cat brain to support the stimulus-evoked enhancement in ATP production/consumption associated with the increased neuronal activity in the activated V1 region. Unlike previous studies, which relied on BOLD modeling to assess the relative (or percent) $CMRO_2$ changes induced by brain stimulation (Davis *et al*, 1998;Hoge *et al*, 1999;Kim *et al*, 1999), the present study directly imaged the absolute $CMRO_2$ values under both resting and activated brain states, which provide not only a quantitative measure of percent $CMRO_2$ change elevated by visual stimulation but also crucial information regarding the relationship between the absolute $CMRO_2$ change and increased brain activity during activation. The finding of significant $CMRO_2$ increase in the activated brain region observed in the present study reveals a tight neurometabolic coupling during brain activation; suggesting the vital role of oxygen metabolism in supporting the intensified neuronal activity in a working brain.

Total Brain Energy Expenditure During Brain Activation

Interestingly, we also consistently detected a $CMRO_2$ decrease in the brain region surrounding the territory showing positive $CMRO_2$ or BOLD change in the cat V1. This phenomenon was observed in all cats, and the functional metabolic $CMRO_2$ image results from two representative cats are shown in Figure 4. When both positive and negative $CMRO_2$ alterations were counted and spatially averaged, the net $CMRO_2$ increase induced by visual stimulation reduced to 9.7% ± 1.9% (n = 6, see Figure 2C) compared with the resting $CMRO_2$ value measured from the same brain regions showing either a significant positive or negative $CMRO_2$ alteration during the visual stimulation; the stimulus-evoked $CMRO_2$ increase was still statistically significant ($P < 0.005$, paired t-test). This finding reveals that the stimulus-evoked $CMRO_2$ change varied significantly across the examined brain regions and consistently displayed two distinct response patterns with positive and negative $CMRO_2$ alterations in the cat brain during visual stimulation.

Similar spatial characteristics have been shown by other physiologic measurements based on the hemodynamic changes of CBV and CBF or BOLD contrast. For instance, negative CBV changes surrounding the central visual cortical regions showing stimulus-evoked increases in CBV were previously reported in the cat brain (Harel *et al*, 2002); and negative changes bordering on the territory of positive changes in BOLD and CBF maps were also observed in the human brain during retinotopic visual stimulation (Shmuel *et al*, 2002). In the latter, BOLD modeling was used to argue that the negative CBF/BOLD changes could correspond to a decrease in $CMRO_2$ in these brain regions; however, ambiguities in the BOLD modeling was recognized and only a qualitative conclusion was reached (Shmuel *et al*, 2002).

Our results suggest that $CMRO_2$ indeed decreases in the brain regions surrounding the primary foci of increased activity, suggesting that the neuronal activity in the regions with negative $CMRO_2$ change might be suppressed owing to a tight neurometabolic coupling. Consistent with this notion, reduction in electrophysiologic signals of neuronal activity was recently reported in the negative BOLD regions surrounding the activated visual cortex in the primate (Shmuel *et al*, 2006). Therefore, these collective lines of evidence suggest that there are similar trends among $CMRO_2$, CBF, CBV, and neuronal activity changes in response to visual stimulation in both activated cortical region and surrounding deactivated cortical region, indicating that a tight coupling among the metabolic and hemodynamic responses to neuronal activity change might qualitatively hold under both activated and deactivated conditions (Raichle and Mintun, 2006).

The negative $CMRO_2$ changes observed during visual stimulation in this study could be driven by oxidative metabolic, other physiologic or neuronal process. Irrespective of the operative mechanism, however, this observed $CMRO_2$ phenomenon may arise to limit total brain energy expenditure superimposed on an expensive energy budget used at the resting state, for instance, to maintain the resting brain network and neuronal connectivity sustained by spontaneous neuronal activity rhythm (Buzsaki and Draguhn, 2004; Fox *et al*, 2006) and to provide a significant amount of 'house-keeping' ATP energy (Du *et al*, 2008). This means that a resting brain is not truly at 'rest' and it costs sizeable brain energy. Thus, the increased energy demand in the activated brain regions could be partially compensated by the reduction of energy usage in other brain regions, leading to a smaller extent of total (or global) brain $CMRO_2$ increase during activation. This energy compensation mechanism could provide a satisfactory explanation for the observation in the present study as well as to the surprising finding from a well-documented work published in 1955, showing no global $CMRO_2$ change in the human brain during an intense mental arithmetic task (Sokoloff *et al*, 1955). Two speculations were discussed in this early publication to interpret the finding: one was that the total energy requirements of the brain, as reflected by the cerebral oxygen consumption, may be independent of the brain activity change elevated by task performance; the other speculation was that the task performance may lead to a spatial redistribution of neuronal and metabolic activities, that is, brain regions with increased functional and metabolic activities could then be counterbalanced by regions of reduced activities so that the global $CMRO_2$ is unchanged (Sokoloff *et al*, 1955). Nevertheless, it was difficult to justify these two possibilities by the global $CMRO_2$ measurements (Sokoloff *et al*, 1955) because lack of information regarding the spatial distribution of positive and negative $CMRO_2$ changes inside the brain. The results from the present study provide vital evidence suggesting that the increased neuronal activity evoked by brain stimulation requires a significantly higher energy demand of oxygen consumption in the activated brain regions than that at rest; however, this increased regional energy demand could be partially compensated by the reduction of energy demand in other brain regions resulting in a smaller increase in $CMRO_2$ over a larger brain volume. This mechanism could be critical for maintaining normal, sustained brain activation in a working brain.

Although, the present study is unable to examine whether the metabolic activity itself or neuronal activity is the primary origin driving the $CMRO_2$ suppression in the surrounding brain regions during visual activation, it has been suggested that the decrease of $CMRO_2$ likely indicates regional depression of synaptic activity (Pasley *et al*, 2007; Seitz and Roland, 1992; Shmuel *et al*, 2006).

One important implication of both negative and positive $CMRO_2$ alterations in the nearby brain regions during stimulation as observed in this study is that the averaged stimulus-evoked $CMRO_2$ change (in either relative or absolute scale) becomes substantially smaller when the spatial resolution of $CMRO_2$ imaging is inadequate to differentiate the regions showing negative and positive $CMRO_2$ alterations; with increased imaging voxel size (i.e., reducing

spatial resolution) and increased partial volume effect, the change in $CMRO_2$ may even become undetectable. This observation could provide key for potentially reconciling the long-standing controversy in the literature regarding the essential questions: if, and how much $CMRO_2$ changes in response to brain stimulation; and whether the oxygen metabolism is vital in supporting brain work (Barinaga, 1997).

It is interesting to note that although the negative $CMRO_2$ (this study) and CBV (Harel *et al*, 2002) changes were observed in the surrounding regions of cat visual cortex, the negative BOLD was not robustly seen in all cats in our study. This observation suggests the complexity of the BOLD signal nature owing to its dependence on the interplay among three stimulus-evoked physiologic parameter (i.e., $CMRO_2$, CBF, and CBV) changes as well as on the baseline levels of these parameters as discussed in the following section. Thus, a single $CMRO_2$ parameter may provide a better and more quantitative measure reflecting the brain energy state or the corresponding neuronal activity level if the limited ^{17}O detection sensitivity is not a major concern; and it should be useful for understanding many neuroscience questions, for example, the relationship between brain energy usage and neuronal excitation versus neuronal inhibition (Buzsaki *et al*, 2007).

Importance of Baseline Cerebral Metabolic Rate of Oxygen

Another striking observation in the present study is that the positive percent $CMRO_2$ changes evoked by visual stimulation were negatively correlated with their corresponding baseline $CMRO_2$ values, as shown in Figure 3C. This finding indicates a strong influence of baseline metabolic activity level on the percent $CMRO_2$ change in response to brain stimulation (Hyder *et al*, 2002; Pasley *et al*, 2007; Shulman *et al*, 2007); thus, the stimulus-evoked percent $CMRO_2$ change alone can become less significant for quantitatively interpreting and fully understanding the neurometabolic relationship if the baseline $CMRO_2$ is not determined.

According to the trend shown in Figure 3C, we could further speculate that the stimulus-evoked $CMRO_2$ percentage change in the awake brains would be less pronounced as compared with the anesthetized brains because a higher baseline level of $CMRO_2$ is expected under the awake state. The visual cortex of the awake human, for instance, has a relatively higher baseline $CMRO_2$ value of ~1.7 μmol/g per min (Fox *et al*, 1988) compared with the value of 0.97 μmol/g per min in the anesthetized cat visual cortex as measured in the present study. On the basis of Figure 3C and the assumption of similar $CMRO_2$ change behaviors between the human and cat visual cortices in response to visual stimulation, one could expect that the percent $CMRO_2$ increase in the human visual cortex during visual stimulation should be significantly less than 32% observed in the anesthetized cat brain in this study, and certainly substantially smaller than the CBF change of 40% to 50% in the human visual cortex (Fox *et al*, 1988; Zhu *et al*, 1998). This notion is consistent with the fact that a hyperoxygenation level in the blood is elevated in the activated brain region because the mismatched $CMRO_2$ and CBF changes, leading to a positive BOLD contrast in fMRI (Ogawa *et al*, 1990). This estimated range of percent $CMRO_2$ increase in response to visual stimulation is also qualitatively consistent with the literature results reporting a wide range from 5% to 30% in the human visual cortex (Chen *et al*, 2001; Davis *et al*, 1998; Fox *et al*, 1988; Hoge *et al*, 1999; Kim *et al*, 1999). However, ultimately studies under the awake state either with the ^{17}O $CMRO_2$ imaging methodology or using this methodology as a calibration for BOLD modeling (Davis *et al*, 1998; Hoge *et al*, 1999; Kim *et al*, 1999; Ogawa *et al*, 1993) will be necessary to draw definitive conclusions in the human brain.

The possible mechanism to link the negative correlation between the stimulus-evoked percent $CMRO_2$ change and its baseline $CMRO_2$ level shown in Figure 3C can be explained by two possible models with distinct assumptions. The first one assumes that $CMRO_2$ can rise from its baseline level to a higher and constant level in the activated brain region during stimulation

(Hyder *et al*, 2002; Pasley *et al*, 2007) so that the absolute stimulus-evoked $CMRO_2$ becomes independent of the baseline $CMRO_2$ level. In this case, a relatively low baseline $CMRO_2$ level should result in a larger stimulus-evoked percent increase in $CMRO_2$; this is consistent with the negative correlation in Figure 3C. The second model is to assume that $CMRO_2$ can rise from its baseline level to a higher level but with a constant $CMRO_2$ increment in the activated brain region. On the basis of this model, the stimulus-evoked percent $CMRO_2$ increase will be larger again if the baseline $CMRO_2$ level is relatively low; this scenario will also lead to a similar negative correlation as shown in Figure 3C. Owing to the inevitable variation among animals in the $CMRO_2$ data measured in the present study, these two models are difficult to be justified with statistical confidence; although the first model was slightly favored by our data showing a relatively smaller intersubject variation (quantified by s.d.) in the absolute values of stimulus-evoked $CMRO_2$ compared with that of stimulus-evoked $CMRO_2$ increments.

The tight correlation between the percent $CMRO_2$ change and baseline $CMRO_2$ level as shown in Figure 3C has several profound impacts on both fMRI methodology and functional brain electrophysiology. First, the percent change of stimulus-evoked $CMRO_2$ can vary as a function of baseline $CMRO_2$ level, and the influence of relative (percent) $CMRO_2$ change on the percent change of BOLD signal measured by fMRI could rely on the baseline $CMRO_2$ level, which can vary substantially among subjects or between awaked and anesthetized brains. Therefore, it is critical to consider the implication of baseline $CMRO_2$ level on quantifying the *relative* changes of stimulus-evoked $CMRO_2$ and/or BOLD (Pasley *et al*, 2007; Shulman *et al*, 2007). Second, the correlation shown in Figure 3C implies that a large portion of brain energy consumption remains in a resting brain. This resting brain energy expenditure should be essential for supporting spontaneous brain activity, coherent neuronal activity rhythm, neurotransmission cycling, and other neuronal signaling processes; and it could be superimposed on the extra stimulus-evoked energy change to perform brain work appropriately. This energy cost could also be crucial for supporting the resting brain network and neuronal connectivity sustained by spontaneous neuronal activity rhythm (Buzsaki and Draguhn, 2004; Fox *et al*, 2006), which has been linked to the slow frequency BOLD signal fluctuation for obtaining functional connectivity maps in a resting brain (Biswal *et al*, 1995; Fox and Raichle, 2007).

The overall findings lead to an important conclusion that both baseline and stimulus-evoked brain energies should be vital for normal brain function in performing specific tasks, and the fraction of these two brain energy expenditures relies on the baseline metabolic activity level, which could be susceptible among subjects, species, and physiologic/pathologic conditions; and the baseline level can also be manipulated readily by varying experimental conditions, for instance, by changing anesthetic depth. The isoflurane anesthetic applied in the present study could significantly low the baseline $CMRO_2$ activity level in the cat visual cortex, ultimately, lead to a relatively larger increase in the percent $CMRO_2$ change and a large absolute $CMRO_2$ increment during brain stimulation as compared with the waked brain state. If the basal $CMRO_2$ level can be further suppressed by using different anesthetic, for example, α-chloralose (Ueki *et al*, 1992), the percent $CMRO_2$ increase could be even larger. Thus, the stimulus-evoked percent $CMRO_2$ change is sensitive to the baseline $CMRO_2$ level and can cover a wide range from deeply anesthetized to awaked brains. This notion provides an explanation to the large discrepancy of the $CMRO_2$ percentage changes reported in the literature (e.g., Fox *et al*, 1988; Hyder *et al*, 2001).

In addition, our results suggest that both baseline $CMRO_2$ level and the stimulus-evoked percent $CMRO_2$ change are equally important for brain to work properly. Although the baseline $CMRO_2$ level can be easily modulated, the total brain energy may have to be resumed and

integrated for supporting brain activation during stimulation if the involved neurons can fully response to the stimulus.

Advantages and Promise of ^{17}O-Based Cerebral Metabolic Rate of Oxygen Imaging Method

Overall findings in this study offer new insights into the underlying physiology of cerebral oxidative metabolism and its essential role in bioenergetics associated with brain activation; they also provide possible clarifications to a number of long-standing neuroscience questions. Moreover, they also highlight the importance of the neuroimaging capability to noninvasively imaging absolute $CMRO_2$ values under both resting and activated brain states with adequate spatial resolution, for instance, to differentiate different brain regions with positive and negative $CMRO_2$ changes in response to visual stimulation as illustrated in this study (Figure 4). This ability is crucial to quantitatively investigate the coupling relationship between the stimulus-evoked neuronal and oxidative metabolic activities. The high-field *in vivo* ^{17}O MRSI approach for 3D mapping of absolute $CMRO_2$ and its change provides a useful neuroimaging modality with satisfactory capability. In this study, we present the first exploration of this promising neuroimaging approach for noninvasively obtaining 3D functional $CMRO_2$ maps in the cat brain during visual stimulation. The results clearly show the advantages of this approach in several aspects. First, the spatially averaged resting $CMRO_2$ value (0.97 ± 0.04 μmol/g per min) measured in the isoflurane anesthetized cat V1 region in this study is in agreement with the value of 1.02 μmol/g per min reported in the literature (Todd and Drummond, 1984), which was measured in the cats under a similar anesthesia condition using the ‘golden-standard’ Kety–Schmidt method. Second, paired $CMRO_2$ imaging measurements performed twice under resting and stimulated conditions in one cat (Cat 5) during the same experimental session show an excellent level of reproducibility for imaging $CMRO_2$ under both conditions (see Figure 3A). This result suggests that the ^{17}O MRSI detection sensitivity offered by high field is adequate for obtaining reliable 3D functional metabolic $CMRO_2$ maps based on only two paired measurements: one under resting and another under stimulation, without averaging from repeated experiments. Third, based only on paired $CMRO_2$ imaging measurements, functional metabolic activation maps of $CMRO_2$ change were obtained reliably in all animals studied. Fourth, the spatial resolution of 3D $CMRO_2$ image achieved in this study was able to provide distinct characteristics of $CMRO_2$ changes in different brain regions in response to brain stimulation in a relatively small animal model. Another and perhaps the most important one is the merits of noninvasiveness, simplicity, robustness, and fair temporal resolution (a few minutes) offered by the high-field *in vivo* ^{17}O MRSI approach, which should hold great promise for numerous biomedical applications beyond healthy subjects and normal brain function research.

Owing to the large differences in spatial resolution and voxel shape between the functional $CMRO_2$ and BOLD maps in the present study, the investigation for correlating the stimulus-evoked $CMRO_2$ change and BOLD signal was not pursued in this study. Nevertheless, the superior quality of high-field *in vivo* ^{17}O MRSI approach for imaging $CMRO_2$ change as shown in this study should be readily combined with MR-based functional imaging approaches for mapping BOLD, CBF, and CBV changes in the same animal model. This ability will provide a unique opportunity for further studying the implications of stimulus-evoked $CMRO_2$ change on neuroimaging signals, in particular, on the BOLD signal; and for improving the reliability of BOLD calibration methods to estimate the percent $CMRO_2$ change (Buxton *et al*, 2004; Davis *et al*, 1998; Hoge *et al*, 1999; Kim *et al*, 1999; Ogawa *et al*, 1993).

Acknowledgements

This work was supported in part by NIH Grants NS41262, EB00329, EB00513, P41 RR08079, and P30NS057091; the Keck foundation.

References

Arai T, Nakao S, Mori K, Ishimori K, Morishima I, Miyazawa T, Fritz-Zieroth B. Cerebral oxygen utilization analyzed by the use of oxygen-17 and its nuclear magnetic resonance. Biochem Biophys Res Commun 1990;169:153–158. [PubMed: 2350339]

Attwell D, Laughlin SB. An energy budget for signaling in the grey matter of the brain. J Cereb Blood Flow Metab 2001;21:1133–1145. [PubMed: 11598490]

Bandettini PA, Wong EC, Hinks RS, Tikofsky RS, Hyde JS. Time course EPI of human brain function during task activation. Magn Reson Med 1992;25:390–397. [PubMed: 1614324]

Barinaga M. What makes brain neurons run? Science 1997;276:196–198. [PubMed: 9132940]

Biswal B, Yetkin FZ, Haughton VM, Hyde JS. Functional connectivity in the motor cortex of resting human brain using echo-planar MRI. Magn Reson Med 1995;34:537–541. [PubMed: 8524021]

Buxton RB, Uludag K, Dubowitz DJ, Liu TT. Modeling the hemodynamic response to brain activation. Neuroimage 2004;23:S220–S233. [PubMed: 15501093]

Buzsaki G, Draguhn A. Neuronal oscillations in cortical networks. Science 2004;304:1926–1929. [PubMed: 15218136]

Buzsaki G, Kaila K, Raichle M. Inhibition and brain work. Neuron 2007;56:771–783. [PubMed: 18054855]

Chen W, Zhu XH, Gruetter R, Seaquist ER, Ugurbil K. Study of oxygen utilization changes of human visual cortex during hemifield stimulation using ^{1}H-{^{13}C} MRS and fMRI. Magn Reson Med 2001;45:349–355. [PubMed: 11241689]

Davis TL, Kwong KK, Weisskoff RM, Rosen BR. Calibrated functional MRI: mapping the dynamic of oxidative metabolism. Proc Natl Acad Sci USA 1998;95:1834–1839. [PubMed: 9465103]

Du F, Zhu XH, Zhang Y, Friedman M, Zhang N, Ugurbil K, Chen W. Tightly coupled brain activity and cerebral ATP metabolic rate. Proc Natl Acad Sci USA 2008;105:6409–6414. [PubMed: 18443293]

Fox MD, Raichle ME. Spontaneous fluctuations in brain activity observed with functional magnetic resonance imaging. Nat Rev Neurosci 2007;8:700–711. [PubMed: 17704812]

Fox MD, Snyder AZ, Zacks JM, Raichle ME. Coherent spontaneous activity accounts for trial-to-trial variability in human evoked brain responses. Nat Neurosci 2006;9:23–25. [PubMed: 16341210]

Fox PT, Raichle ME, Mintun MA, Dence C. Nonoxidative glucose consumption during focal physiologic neural activity. Science 1988;241:462–464. [PubMed: 3260686]

Harel N, Lee SP, Nagaoka T, Kim DS, Kim SG. Origin of negative blood oxygenation level-dependent fMRI signals. J Cereb Blood Flow Metab 2002;22:908–917. [PubMed: 12172376]

Hendrich K, Hu X, Menon R, Merkle H, Camarata P, Heros R, Ugurbil K. Spectroscopic imaging of circular voxels with a two-dimensional Fourier-Series Window technique. J Magn Reson 1994;105:225–232.

Hoge RD, Atkinson J, Gill B, Crelier GR, Marrett S, Pike GB. Linear coupling between cerebral blood flow and oxygen consumption in activated human cortex. Proc Natl Acad Sci USA 1999;96:9403–9408. [PubMed: 10430955]

Hyder F, Kida I, Behar KL, Kennan RP, Maciejewski PK, Rothman DL. Quantitative functional imaging of the brain: towards mapping neuronal activity by BOLD fMRI. NMR Biomed 2001;14:413–431. [PubMed: 11746934]

Hyder F, Patel AB, Gjedde A, Rothman DL, Behar KL, Shulman RG. Neuronal-glial glucose oxidation and glutamatergic-GABAergic function. J Cereb Blood Flow Metab 2006;26:865–877. [PubMed: 16407855]

Hyder F, Rothman DL, Shulman RG. Total neuroenergetics support localized brain activity: implications for the interpretation of fMRI. Proc Natl Acad Sci USA 2002;99:10771–10776. [PubMed: 12134057]

Ibaraki M, Miura S, Shimosegawa E, Sugawara S, Mizuta T, Ishikawa A, Amano M. Quantification of cerebral blood flow and oxygen metabolism with 3-dimensional PET and 15O: validation by comparison with 2-dimensional PET. J Nucl Med 2008;49:50–59. [PubMed: 18077532]

Kim SG, Rostrup E, Larsson HB, Ogawa S, Paulson OB. Determination of relative $CMRO_2$ from CBF and BOLD changes: significant increase of oxygen consumption rate during visual stimulation. Magn Reson Med 1999;41:1152–1161. [PubMed: 10371447]

Kwong KK, Belliveau JW, Chesler DA, Goldberg IE, Weisskoff RM, Poncelet BP, Kennedy DN, Hoppel BE, Cohen MS, Turner R, Cheng HM, Brady TJ, Rosen BR. Dynamic magnetic resonance imaging of human brain activity during primary sensory stimulation. Proc Natl Acad Sci USA 1992;89:5675–5679. [PubMed: 1608978]

Lei H, Ugurbil K, Chen W. Measurement of unidirectional Pi to ATP flux in human visual cortex at 7 T by using *in vivo* ^{31}P magnetic resonance spectroscopy. Proc Natl Acad Sci USA 2003;100:14409–14414. [PubMed: 14612566]

Mateescu, GD.; Yvars, GM.; Maylish-Kogovsek, L.; LaManna, JC.; Lust, WD.; Sudilovsky, D. Oxygen-17 MRI and MRS of the brain, the heart and coronary arteries; Proceeding of Annual Meeting of Society of Magnetic Resonance in Medicine, Amsterdam, the Netherlands; 1989. p. 650

Mintun MA, Raichle ME, Martin WR, Herscovitch P. Brain oxygen utilization measured with O-15 radiotracers and positron emission tomography. J Nucl Med 1984;25:177–187. [PubMed: 6610032]

Mintun MA, Vlassenko AG, Shulman GL, Snyder AZ. Time-related increase of oxygen utilization in continuously activated human visual cortex. Neuroimage 2002;16:531–537. [PubMed: 12030835]

Ogawa S, Lee T-M, Kay AR, Tank DW. Brain magnetic resonance imaging with contrast dependent on blood oxygenation. Proc Natl Acad Sci USA 1990;87:9868–9872. [PubMed: 2124706]

Ogawa S, Menon RS, Tank DW, Kim S-G, Merkle H, Ellermann JM, Ugurbil K. Functional brain mapping by blood oxygenation level-dependent contrast magnetic resonance imaging. Biophys J 1993;64:800–812.

Ogawa S, Tank DW, Menon R, Ellermann JM, Kim S-G, Merkle H, Ugurbil K. Intrinsic signal changes accompanying sensory stimulation: functional brain mapping with magnetic resonance imaging. Proc Natl Acad Sci USA 1992;89:5951–5955. [PubMed: 1631079]

Pasley BN, Inglis BA, Freeman RD. Analysis of oxygen metabolism implies a neural origin for the negative BOLD response in human visual cortex. Neuroimage 2007;36:269–276. [PubMed: 17113313]

Pekar J, Ligeti L, Ruttner Z, Lyon RC, Sinnwell TM, van Gelderen P, Fiat D, Moonen CT, McLaughlin AC. *In vivo* measurement of cerebral oxygen consumption and blood flow using ^{17}O magnetic resonance imaging. Magn Reson Med 1991;21:313–319. [PubMed: 1745131]

Raichle, ME. Circulatory and metabolic correlates of brain function in normal humans. In: Mountcastle, VB.; Plum, F.; Geiger, SR., editors. Handbook of physiology-the nervous system. Bethesda: American Physiological Society; 1987. p. 643-674.

Raichle ME, Mintun MA. Brain work and brain imaging. Annu Rev Neurosci 2006;29:449–476. [PubMed: 16776593]

Seitz RJ, Roland PE. Vibratory stimulation increases and decreases the regional cerebral blood flow and oxidative metabolism: a positron emission tomography (PET) study. Acta Neurol Scand 1992;86:60–67. [PubMed: 1519476]

Shmuel A, Augath M, Oeltermann A, Logothetis NK. Negative functional MRI response correlates with decreases in neuronal activity in monkey visual area V1. Nat Neurosci 2006;9:569–577. [PubMed: 16547508]

Shmuel A, Yacoub E, Pfeuffer J, Van de Moortele PF, Adriany G, Hu X, Ugurbil K. Sustained negative BOLD, blood flow and oxygen consumption response and its coupling to the positive response in the human brain. Neuron 2002;36:1195–1210. [PubMed: 12495632]

Shulman RG, Rothman DL, Hyder F. A BOLD search for baseline. Neuroimage 2007;36:277–281. [PubMed: 17223362]

Sokoloff, L. Relationship between functional activity and energy metabolism in the nervous system: whether, where and why?. In: Lassen, NA.; Ingvar, DH.; Raichle, ME., et al., editors. Brain work and mental activity. Copenhagen: Munksgaard; 1991. p. 52-64.

Sokoloff L, Mangold R, Wechsler RL, Kenney C, Kety SS. The effect of mental arithmetic on cerebral circulation and metabolism. J Clin Invest 1955;34:1101–1108. [PubMed: 14392225]

Todd MM, Drummond JC. A comparison of the cerebrovascular and metabolic effects of halothane and isoflurane in the cat. Anesthesiology 1984;60:276–282. [PubMed: 6703382]

Ueki M, Mies G, Hossmann KA. Effect of alpha-chloralose, halothane, pentobarbital and nitrous oxide anesthesia on metabolic coupling in somatosensory cortex of rat. Acta Anaesthesiol Scand 1992;36:318–322. [PubMed: 1595336]

Xiong J, Gao JH, Lancaster JL, Fox PH. Clustered pixels analysis for functional MRI activation studies of the human brain. Hum Brain Mapp 1995;3:287–301.

Zhang N, Zhu XH, Lei H, Ugurbil K, Chen W. Simplified methods for calculating cerebral metabolic rate of oxygen based on ^{17}O magnetic resonance spectroscopic imaging measurement during a short $^{17}O_2$ inhalation. J Cereb Blood Flow Metab 2004;24:840–848. [PubMed: 15362714]

Zhu XH, Kim SG, Andersen P, Ogawa S, Ugurbil K, Chen W. Simultaneous oxygenation and perfusion imaging study of functional activity in primary visual cortex at different visual stimulation frequency: quantitative correlation between BOLD and CBF changes. Magn Reson Med 1998;40:703–711. [PubMed: 9797153]

Zhu XH, Zhang N, Zhang Y, Zhang X, Ugurbil K, Chen W. *In vivo* ^{17}O NMR approaches for brain study at high field. NMR Biomed 2005;18:83–103. [PubMed: 15770611]

Zhu XH, Zhang Y, Tian RX, Lei H, Zhang N, Zhang X, Merkle H, Ugurbil K, Chen W. Development of ^{17}O NMR approach for fast imaging of cerebral metabolic rate of oxygen in rat brain at high field. Proc Natl Acad Sci USA 2002;99:13194–13199. [PubMed: 12242341]

Zhu XH, Zhang Y, Zhang N, Ugurbil K, Chen W. Noninvasive and three-dimensional imaging of $CMRO_2$ in rats at 9.4 T: reproducibility test and normothermia/ hypothermia comparison study. J Cereb Blood Flow Metab 2007;27:1225–1234. [PubMed: 17133228]

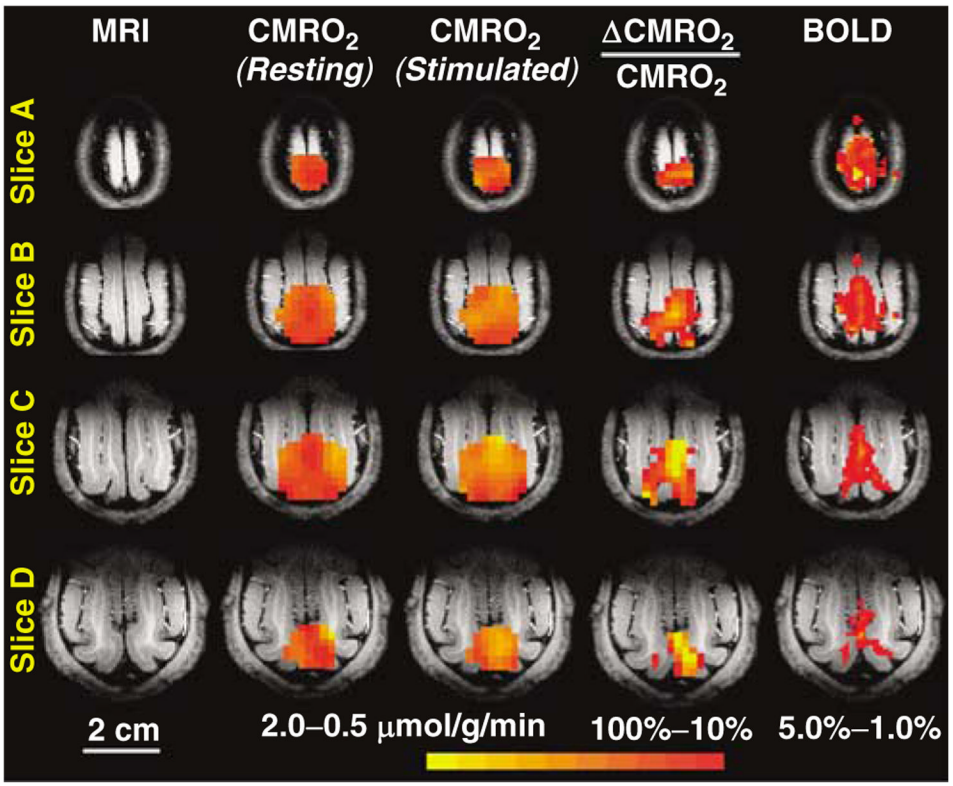

Figure 1.

Significant $CMRO_2$ increase in activated visual cortex. Three-dimensional $CMRO_2$ maps obtained at resting (second column from the left) and stimulated (third column) conditions; 3D functional metabolic activation maps showing percent changes of $CMRO_2$ elevated by visual stimulation (fourth column); BOLD-based fMRI maps (fifth column); and anatomic brain images (first column) in four adjacent image slices from a representative cat brain.

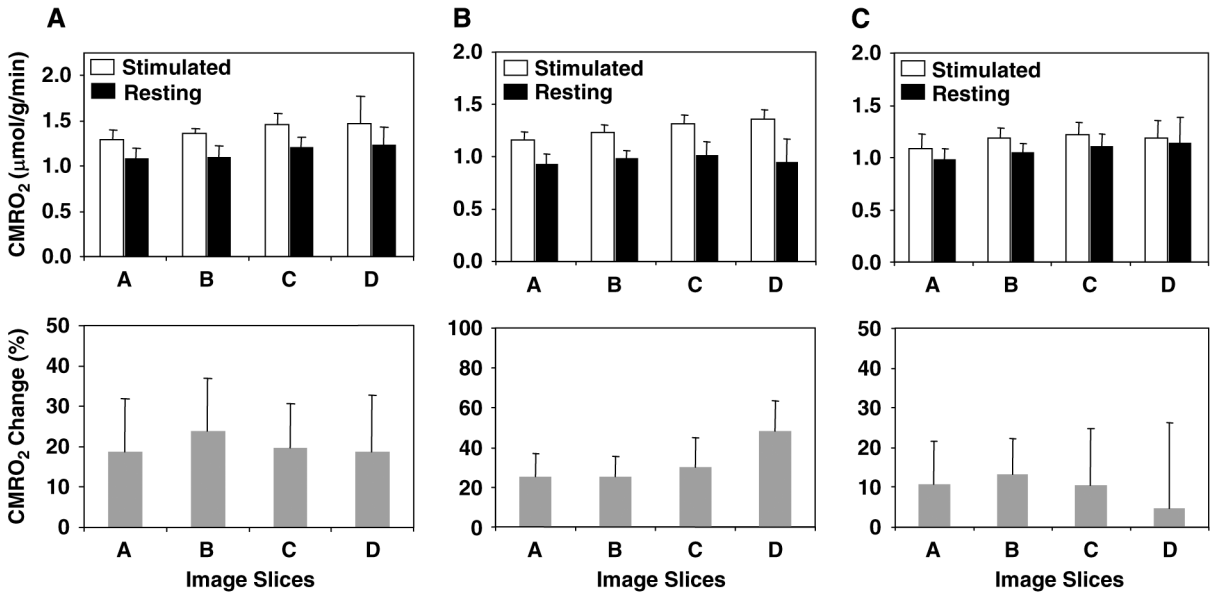

Figure 2.

Summary of resting and activated $CMRO_2$ and percent changes. Summarized absolute $CMRO_2$ values measured at resting and during visual stimulation (top inserts) and their percent changes (bottom inserts) from four $CMRO_2$ image slices covering the visual cortex of cat anesthetized with isoflurane. (**A**) Results from a representative cat. (**B**) Averaged results from six experiments, for the ^{17}O MRSI voxels with only positive $CMRO_2$ change. (**C**) Averaged results from six experiments for the ^{17}O MRSI voxels with both positive and negative $CMRO_2$ changes. Paired *t*-test indicates a statistically significant difference between the control and activated $CMRO_2$ values ($P < 0.005$ using paired *t*-test for both panels B and C).

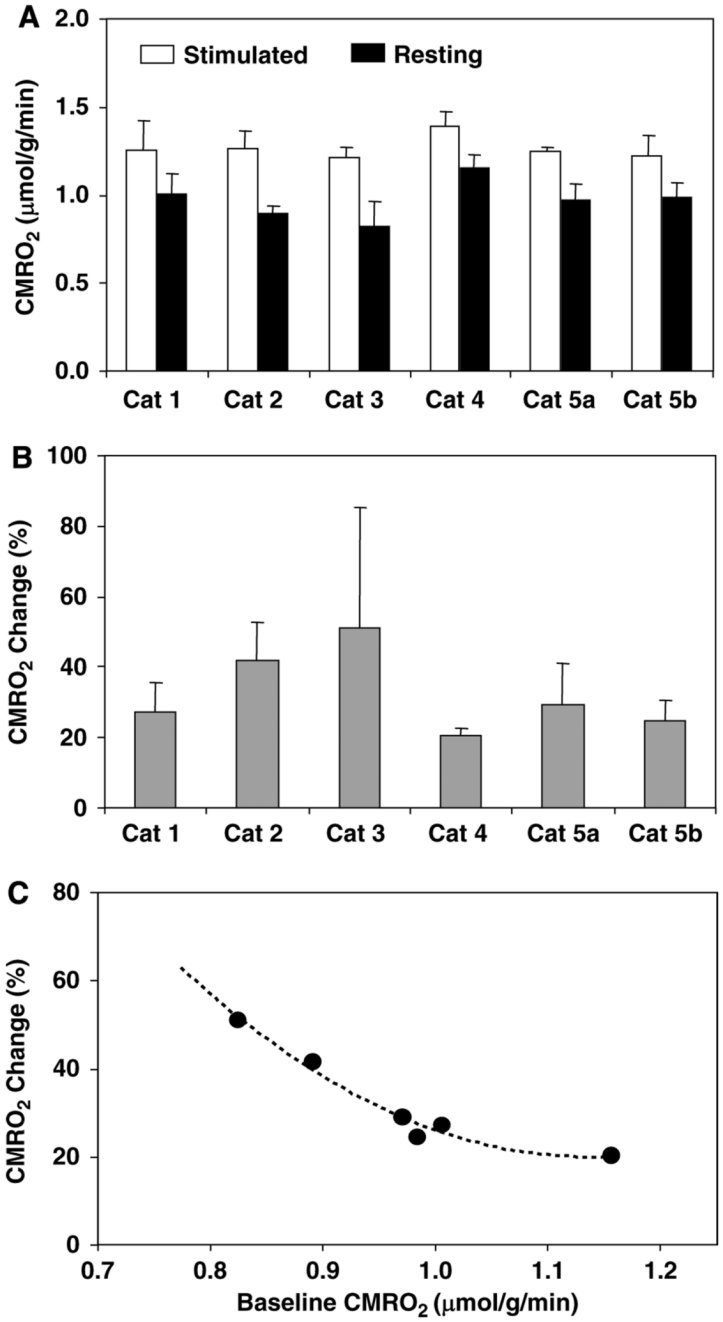

Figure 3.

Stimulus-evoked $CMRO_2$ increase and its relation to resting $CMRO_2$. (**A**) Averaged absolute $CMRO_2$ values for each cat brain at resting and during visual stimulation. (**B**) The averaged percent $CMRO_2$ increases elevated by visual stimulation. (**C**) The negative correlation between the percent $CMRO_2$ changes and baseline $CMRO_2$ values. This figure shows that visual stimulation elevates a significant $CMRO_2$ increase in the activated visual cortex of five cats studied ($P < 0.005$ using paired *t*-test for both panels A and B), and the percent $CMRO_2$ changes are negatively correlated to the corresponding baseline $CMRO_2$ levels.

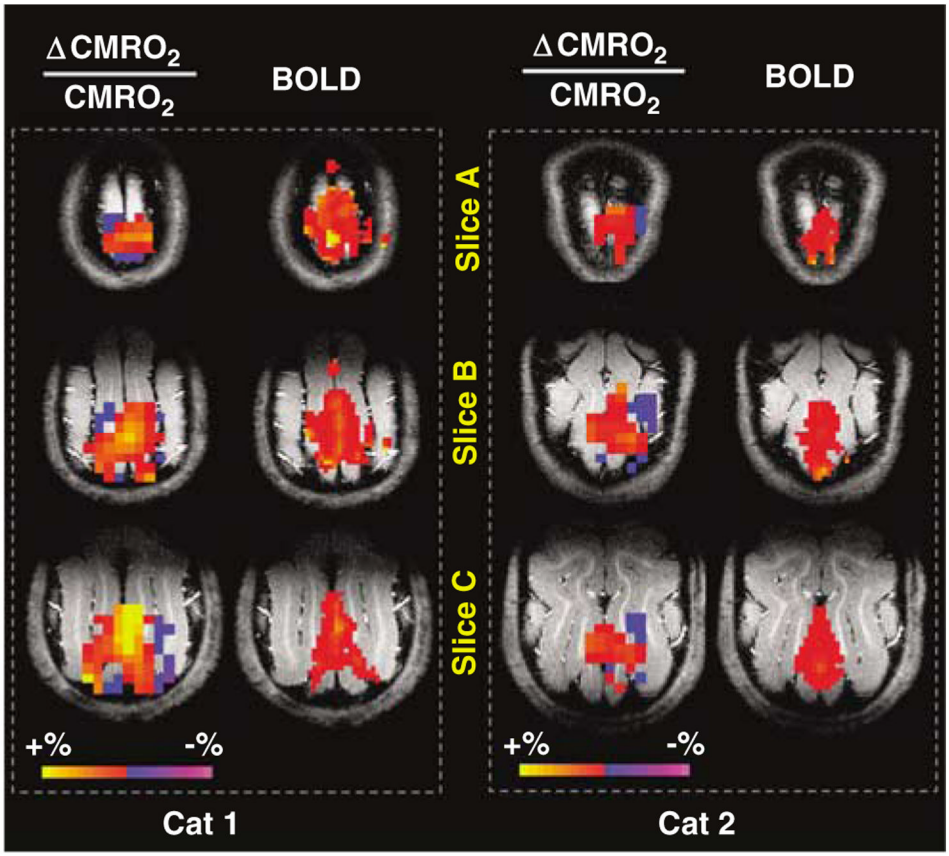

Figure 4.
Spatially compensated $CMRO_2$ changes elevated by brain stimulation. Functional $CMRO_2$ maps (show both positive and negative changes) and fMRI BOLD maps during visual stimulation from two representative cats. This figure shows that the $CMRO_2$ increases in the central activated visual cortex regions are commonly accompanied by $CMRO_2$ decreases in surrounding brain regions.